FTIR Spectroscopy of the K Photointermediate of *Neurospora* Rhodopsin: Structural Changes of the Retinal, Protein, and Water Molecules after Photoisomerization†

Yuji Furutani,[‡,§,⊥] Arandi G. Bezerra Jr.,[||,#] Stephen Waschuk,[||] Masayo Sumii,[‡] Leonid S. Brown,[||] and Hideki Kandori*[,‡,⊥]

Department of Materials Science and Engineering, Nagoya Institute of Technology, Showa-ku, Nagoya 466-8555, Japan, Department of Biophysics, Graduate School of Science, Kyoto University, Sakyo-ku, Kyoto 606-8502, Japan, Department of Physics, University of Guelph, Guelph, Ontario N1G 2W1, Canada, and Core Research for Evolutional Science and Technology (CREST), Japan Science and Technology Corporation, Kyoto 606-8502, Japan

Received April 26, 2004; Revised Manuscript Received June 7, 2004

ABSTRACT: *Neurospora* rhodopsin (NR, also known as NOP-1) is the first rhodopsin of the haloarchaeal type found in eucaryotes. NR demonstrates a very high degree of conservation of the amino acids that constitute the proton-conducting pathway in bacteriorhodopsin (BR), a light-driven proton pump of archaea. Nevertheless, NR does not appear to pump protons, suggesting the absence of the reprotonation switch that is necessary for the active transport. The photocycle of NR is much slower than that of BR, similar to the case of *pharaonis* phoborhodopsin (*p*pR), an archaeal photosensory protein. The functional and photochemical differences between NR and BR should be explained in the structural context. In this paper, we studied the structural changes of NR following retinal photoisomerization by means of low-temperature Fourier transform infrared (FTIR) spectroscopy and compared the obtained spectra with those for BR. For the spectroscopic analysis, we established the light-adaptation procedure for NR reconstituted into 1,2-dimyristoyl-*sn*-glycero- 3-phosphocholine/1,2-dimyristoyl-*sn*-glycero-3-phosphate (DMPC/DMPA) liposomes, which takes approximately 2 orders of magnitudes longer than in BR. The structure of the retinal chromophore and the hydrogen-bonding strength of the Schiff base in NR are similar to those in BR. Unique spectral features are observed for the S−H stretching vibrations of cysteine and amide-I vibrations for NR before and after retinal isomerization. In NR, there are no spectral changes assignable to the amide bands of α helices. The most prominent difference between NR and BR was seen for the water O−D stretching vibrations (measured in D_2O). Unlike for haloarchaeal rhodopsins such as BR and *p*pR, no O−D stretches of water under strong hydrogen-bonded conditions (<2400 cm^{-1}) were observed in the NR_K minus NR difference spectra. This suggests a unique hydrogen-bonded network of the Schiff base region, which may be responsible for the lack of the reprotonation switch in NR.

Neurospora rhodopsin (NR,[1] also known as NOP-1) is a membrane retinal-binding protein, which belongs to the type-I rhodopsin family (*1*). Type-I rhodopsins contain all-*trans*-retinal bound to a lysine side chain roughly in the middle of the seventh transmembrane helix via a protonated Schiff base but are not otherwise homologous to visual pigments (type-II rhodopsins). The retinal chromophore experiences all-trans to 13-cis photoisomerization followed by a chain of thermal relaxations called the photocycle. The protein moiety of type-I rhodopsins responds to the changes in the retinal geometry with its own conformational changes, which serve the purpose of ion transport or signaling (reviewed in ref *2*). The first major function of type-I rhodopsins is ion transport as exemplified by light-driven pumping of protons or chloride. The second major function is photosensory transduction, where optical signals are transformed into conformational changes and communicated to a transducer protein mediating phototaxis or other responses to light. There is also a special case of rhodopsins from *Chlamydomonas*, where the type-I rhodopsin domain is part of a much larger protein in which it regulates passive transport of protons or calcium (*3, 4*).

In the not so distant past, it was believed that type-I rhodopsins were present only in halobacteria, so this protein family is sometimes referred to as rhodopsins of haloarchaeal type (*1*). Halobacterial rhodopsins are very well studied and the halobacterial genome contains genes coding for four

† This work was supported in part by grants from Japanese Ministry of Education, Culture, Sports, Science, and Technology to H.K., by Research Fellowships from the Japan Society for the Promotion of Science for Young Scientists to Y.F., and by the NSERC grant to L.S.B.

* To whom correspondence should be addressed. Phone and Fax: 81-52-735-5207. E-mail: kandori@nitech.ac.jp.

‡ Nagoya Institute of Technology.

§ Kyoto University.

|| University of Guelph.

⊥ CREST.

A. G. Bezerra is on research leave from Departamento de Física, Centro Federal de Educação Tecnológica do Paraná, CEFET-PR, 80230-901 Cutiriba, PR, Brazil.

[1] Abbreviations: NR, *Neurospora* rhodopsin; NR_K, K intermediate of NR; BR, bacteriorhodopsin; BR_K, K intermediate of BR; *p*pR, *pharaonis* phoborhodopsin; HOOP, hydrogen out-of-plane vibration; DMPC, 1,2-dimyristoyl-*sn*-glycero-3-phosphocholine; DMPA, 1,2-dimyristoyl-*sn*-glycero-3-phosphate.

10.1021/bi049158c CCC: $27.50
Published on Web 07/10/2004

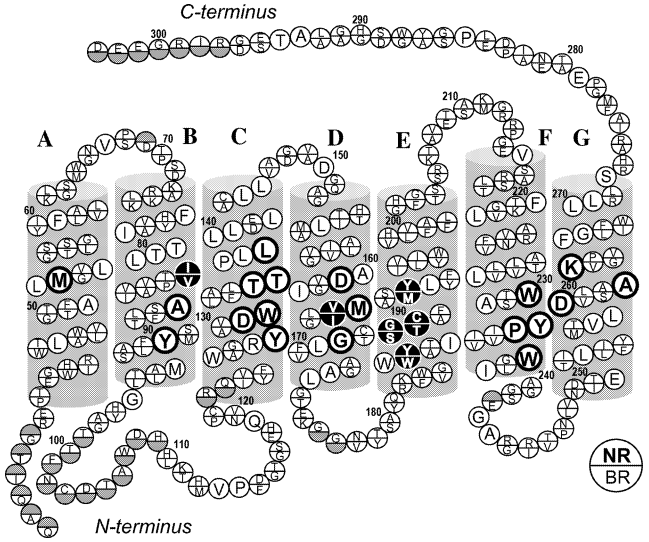

FIGURE 1: Comparison of amino acid sequences of bacteriorhodopsin and the expressed part of NR. The transmembrane topology is based on the crystallographic three-dimensional model of BR (*54*). The sequence alignment was done using CLUSTALW (*63*) with the default settings. Single letters in a circle denote residues common to NR and BR. The residues that are different in NR and BR are denoted at the top and bottom of the circles, respectively. The bold or filled circles compose the retinal-binding site within 5 Å of the chromophore.

related proteins (*5*): bacteriorhodopsin (BR), halorhodopsin (HR), sensory rhodopsin (SR, also called sensory rhodopsin I, SR-I), and phoborhodopsin (pR, also called sensory rhodopsin II, SR-II). BR and HR are light-driven ion pumps, which act as an outward proton pump and an inward Cl^- pump, respectively (*6*−*8*). On the other hand, SR and pR are photoreceptors of halobacteria mediating attractant and repellent responses in phototaxis, respectively (*9*−*11*). Even though physiological and biochemical data suggested that type-I rhodopsins may exist in organisms other than halobacteria, it was only during the last 5 years that several genome sequencing projects have convincingly demonstrated the presence of rhodopsins of haloarchaeal type not only in archaea, but also in bacteria and eukaryota (reviewed in refs *1*, *2*, *12*). Eubacterial rhodopsins were found both in γ and α proteobacteria (*13*, *14*), as well as in cyanobacteria (*15*). In eucaryotes, type-I rhodopsins were found in fungi (*16*), green algae (*3*, *4*), dynoflagellates (*17*), and cryptomonads (*2*).

Neurospora rhodopsin was the first fungal and the first type-I eucaryotic rhodopsin characterized on the genetic level (*16*) and remains the only fungal rhodopsin characterized as a protein (*18*−*20*). More than a dozen of genes for related fungal rhodopsins were discovered since then (*21*−*23*), but their function remains unknown (reviewed in ref *12*). The primary structure of fungal rhodopsins, especially in their putative transmembrane regions, is highly homologous to that of both BR and pR (Figure 1) (*1*, *12*, *16*). Strong conservation of the amino acids involved in proton translocation in BR (especially Asp-85 and Asp-96, respective acceptor and donor of the Schiff base proton) suggested that NR should possess some proton-pumping activity, even though its slow photocycling rate suggested otherwise (*18*). Thus, a more detailed biophysical study was necessary.

NR was heterologously overexpressed in the methylotrophic yeast *Pichia pastoris*, where it inserts into the cell membrane and readily reconstitutes with all-*trans*-retinal to form a red photoactive pigment (*18*). It should be kept in mind that NR may behave somewhat differently in its native lipid environment and in the presence of its possible protein partners. Photochemistry and proton transport activity of wild-type NR and some of its mutants were studied using time-resolved spectroscopy in the visible and infrared, combined with static Raman spectroscopy and proton-pumping assays (*18*−*20*). It was found that both photochemistry and proton kinetics are more similar to those of pR than of BR, suggesting that NR may be a photosensor rather than a pump. The proton kinetics and pumping studies found that the transient proton release and uptake in the NR photocycle did not result in a detectable proton transport (*19*). Time-resolved spectroscopy of NR mutants showed that, even though Asp-131, the homologue of Asp-85 of BR, became protonated in the course of the Schiff base deprotonation (M rise), the reprotonation of the Schiff base did not occur from the homologue of Asp-96 of BR, Glu-142 (*19*, *20*). The existing model of the photocycle of NR assumes that, although it goes through a sequence of photointermediates qualitatively similar to K, L, M, N, and O of BR, there is no net transport of protons, because both H^+ uptake and release happen on the extracellular side of the protein (*19*). This is a very surprising result, taking into account almost complete conservation of the amino acids constituting the proton-conducting pathway in BR and the BR-like retinal configuration in NR as evidenced by the Raman spectra (*19*). The working hypothesis is that NR may not transport protons despite all of the structural similarities with BR because its reprotonation switch is not functional. The latest views on the reprotonation switch mechanism of BR supported by X-ray diffraction data and FTIR spectroscopy stress the importance of strain in the retinal bonds and the interaction of its Schiff base with internal water molecules (*24*, *25*). Thus, if the reprotonation switch is truly dysfunctional in NR, one may expect to see the differences (with respect to BR) in the retinal geometry as well as in its interactions with water upon photoisomerization. In this paper, we studied low-temperature FTIR characteristics of the K intermediate of NR, comparing it with those of BR and paying special attention to the bands of bound water, retinal Schiff base, and retinal skeleton. This study expands FTIR characterization of NR to earlier intermediates complementing the previous reports on late intermediates (*19*, *20*). It reveals important structural differences between the K intermediates of BR and NR, which may eventually shed light on a mechanism of their functional divergence.

MATERIALS AND METHODS

Expression of Neurospora Rhodopsin in P. pastoris. Wild-type His-tagged NR with a truncated N terminus was expressed in *P. pastoris* (the expression system was kindly provided by John and Elena Spudich, University of Texas Medical School, Houston, TX) as described before (*18*) with the following modifications. The cells were harvested 36−42 h after the expression was induced in BMM medium (minimal methanol buffered with phosphate at pH 5.6, methanol concentration 0.7%), because we noticed a steep decrease in the NR concentration when the cells were incubated longer. Additionally, we added all-*trans*-retinal (Sigma Chemicals) directly to the growth medium 24 h after

the induction to a final concentration of ~5 μM. Membranes containing wild-type NR were isolated as described elsewhere (*19*) with the following modifications. Washed *P. pastoris* cells were resuspended in buffer A (7 mM NaH_2PO_4 at pH 6.5, 7 mM EDTA, 7 mM DTT, and 1 mM PMSF) and slowly shaken with all-*trans*-retinal (added to a final concentration of ~50 μM) at room temperature for 3−4 h in the presence of ~20 mg of lyticase (crude, from *Arthrobacter luteus*, Sigma Chemicals) per 1.5 L of cell culture to digest cell walls. Subsequently, the cells were centrifuged at 1500*g* and resuspended in an equal volume of buffer A. The cells were vortexed several times with a 40% volume of glass beads (420−600 μm, acid washed) and centrifuged at low speed (700*g*). The colored supernatant was withdrawn and stored, while the remaining cells and debris were resuspended in a few milliliters of the same buffer, and vortexing followed by centrifugation was repeated several times until the breakage of the cells was complete. The supernatants were combined and centrifuged for 20−30 min at 30000*g* in a fixed-angle rotor, and the resulting red-colored pellets were frozen for later use.

Purification and Reconstitution into Liposomes. The liposomes containing NR were obtained as follows. The NR membrane pellets were resuspended in solubilization buffer (1% Triton X-100 and 20 mM K phosphate at pH 7.5) and stirred for a few hours at room temperature followed by overnight stirring at 4 °C. The solubilization mixture was centrifuged for 20−30 min at 30000*g* in a fixed-angle rotor, the supernatant was stored, and the pellet was re-extracted with the same solubilization buffer if necessary. Combined supernatants were supplemented with 300 mM NaCl, and the solubilized protein was incubated with Ni−NTA agarose (Qiagen) for several hours. The resin with bound NR was repeteadly washed with the solubilization buffer and then treated with the elution buffer (250 mM imidazole, 400 mM NaCl, 50 mM K phosphate, and 0.25% Triton X-100 at pH 7.5), supplemented with polar lipids of *P. pastoris* (0.2 mg/mL in 2% Triton X-100) to stabilize the purified NR. The polar lipids were extracted from *P. pastoris* cells following the protocol of Kates et al. (*26*) with methanol/chloroform extraction followed by acetone precipitation. The purified NR eluate was concentrated using Millipore Ultrafree centrifugal filter devices (cutoff 10 000 Da) at 3700*g* and reconstituted into liposomes following the method of Rigaud et al. (*27*). Briefly, 1,2-dimyristoyl-*sn*-glycero-3-phosphocholine (DMPC) and 1,2-dimyristoyl-*sn*-glycero-3-phosphate (DMPA) (Avanti Lipids) were taken in a 9:1 ratio by weight, dissolved in warm chloroform, thoroughly dried under vacuum, and rehydrated for 1 h in a liposome buffer (150 mM KCl and 1 mM K phosphate at pH 6.8). Multilamellar liposomes formed this way (at a concentration of ~8 mg/mL) were diluted 2-fold with reconstitution buffer (100 mM Na sulfate and 20 mM K phosphate at pH 7.5) and mixed with the purified concentrated NR in a 4:1 lipid/protein ratio by weight. We assumed that 1 OD (1-cm path length) of absorbance of NR at 526 nm originates from 0.5 mg of the protein in 1 mL. The protein−lipid mixture had to be transparent at this point, indicating that the multilamellar liposomes were solubilized. If the solution was not transparent, 2% Triton X-100 was added until most of the turbidity disappeared. After incubation for 10 min, Bio-Beads SM-2 (Bio-Rad) degassed in the reconstitution buffer were added to remove the detergent. We made four additions of Bio-Beads, one every hour, approximately 100 mg per 1 mL of 1% Triton. After incubation for 4 h with the beads, the liquid was removed by a syringe and the liposomes were collected by centrifugation in 100 mM NaCl (30 min at 40000*g*). The liposomes were further washed by additional centrifugations, and the final liposome pellet was frozen for later use.

FTIR Spectroscopy. FTIR spectroscopy was performed as described previously (*28*, *29*) but with the modified light adaptation. The NR sample reconstituted into DMPC/DMPA liposomes was washed 3 times with 2 mM phosphate buffer (pH 7). The pellet was resuspended in the same buffer, and the concentration was adjusted to ~2 OD units at 520 nm per mL. An 80-μL aliquot was deposited on a BaF_2 window of 18-mm diameter and dried in a glass vessel that was evacuated by an aspirator.

The dark-adapted NR contains both 13-*cis*- and all-*trans*-retinal. The light adaptation yielded a spectral red shift of λ_{max} of the visible absorption (from 519 to 532 nm), which accompanied 13-*cis*- to all-*trans*-retinal isomerization. For the NR sample in the DMPC/DMPA liposomes, the light adaptation required continuous illumination for about 1 h with a 500-nm light (through an interference filter 03FIV006, Melles Griot) from a 1-kW halogen−tungsten lamp in a slide projector. We also found that the dark adaptation takes a very long time (about 1 day). Therefore, in our measurements, we first hydrated the NR film with a saturating amount of water and illuminated it for 1 h at room temperature. After the procedure, the NR film was quickly dried and rehydrated with H_2O, D_2O, or $D_2{}^{18}O$. The sample was then placed in a cell in an Oxford DN-1704 cryostat mounted in the Bio-Rad FTS-40 spectrometer. The cryostat was equipped with an Oxford ITC-4 temperature controller, and the temperature was regulated with 0.1 K precision.

Illumination with 500-nm light at 77 or 100 K for 2 min converted NR to NR_K. Because NR_K was completely reconverted to NR upon illumination with >600-nm light for 1 min, as evidenced by the spectral shape, which is a mirror image of that for the NR−NR_K transition, cycles of alternating illumination with 500- and >600-nm light were repeated a number of times. The difference spectrum was calculated from two spectra constructed from 128 interferograms taken before and after the illumination. A total of 24 difference spectra obtained in this way were averaged to produce the NR_K minus NR spectrum. Because linear dichroism experiments revealed random orientation of NR molecules in the liposome film, an IR polarizer was not used.

BR_K minus BR difference spectra were taken from Kandori et al. (*30*) and Tanimoto et al. (*24*). Because BR molecules are highly oriented in the film, unlike NR, the data with a window-tilting angle of 53.5° in polarized FTIR spectroscopy were used for comparison.

Raman-Scattering Spectroscopy. Raman spectra of NR were measured using the Renishaw Raman Imaging Microscope, System 2000 that is located in the Electrochemical Technology Center, University of Guelph, Wellington, Canada. The probe beam was provided by a 27-mW diode laser at 785 nm, and spectral resolution was 1 cm^{-1}. The samples were prepared by drying the buffered liposome suspension on one of the walls of a 1 × 1 cm quartz cuvette. After that, 100−200 μL of H_2O or D_2O was placed inside

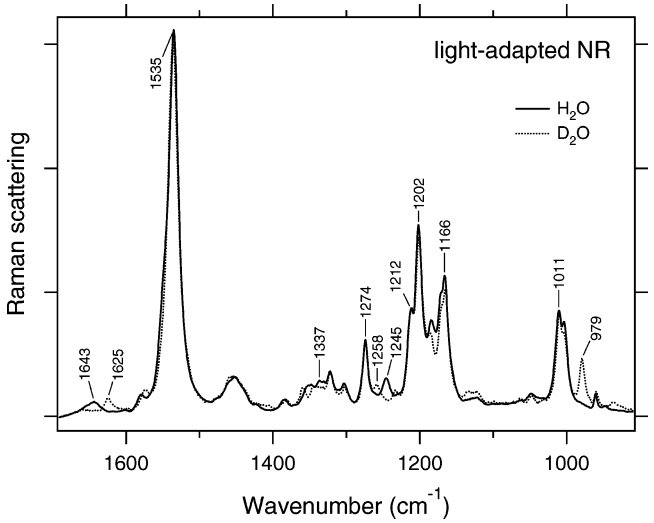

FIGURE 2: Raman scattering (785-nm excitation) spectra of light-adapted NR liposomes measured in H_2O (—) and D_2O (- - -). The bands assignable to retinal are labeled. As described in the Materials and Methods, the Raman bands around 1000 and, in part, 1450 cm^{-1} come from the protein/lipid moiety and are not labeled.

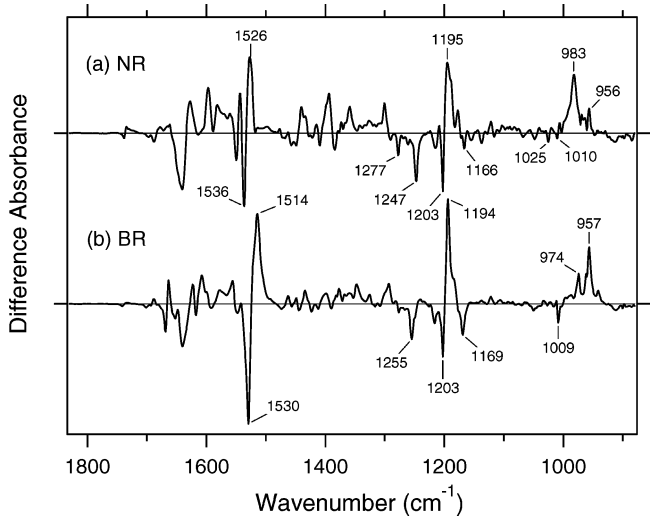

FIGURE 3: NR_K minus NR (a) and BR_K minus BR (b) spectra in the 1830−880 cm^{-1} region measured at pH 7 and 77 K upon hydration with H_2O. In the hydrated film, NR molecules are oriented randomly, while BR molecules are highly oriented. The spectrum in (b) is reproduced from Kandori et al. (*30*), where the sample window is tilted by 53.5°. One division of the *y* axis corresponds to 0.006 absorbance units.

the cuvette, it was sealed, and sufficient time for the vapors to equlibrate was given before the measurements were started (as monitored using Raman lines of H_2O or D_2O). In this sample configuration, the buffer lines are negligible and the whole spectrum is dominated by the scattering from the retinal chromophore with an exception of several minor bands coming from the protein/lipid moiety (most notably at around 1000 and 1450 cm^{-1}, with the latter overlapping with the retinal bands).

RESULTS

Light Adaptation of NR. Dark-adapted NR contains both 13-*cis*- and all-*trans*-retinal (*18*, *19*), similar to the light-driven ion pumps BR and HR but different from the phototaxis proteins pR and sR. All archaeal rhodopsins use all-*trans*-retinal in their functional forms; thus, the light adaptation should be conducted to accumulate it. Under the present experimental conditions, we can light-adapt BR samples by illuminating with >500-nm light for 2 min at 273 K. In contrast, we found that much longer illumination is required for the light adaptation of NR. As described in the Materials and Methods, we illuminated each NR film for 1 h. As a consequence, visible absorption maximum shifted from 519 to 532 nm. It was reported that the NR sample reconstituted with all-*trans*-retinal in the yeast membrane has its absorption maximum at 535 nm (*18*).

The light adaptation process was also monitored by Raman spectroscopy. Dark-adapted NR samples possess the ethylenic C═C stretches at 1535 and 1552 cm^{-1} (data not shown), which correspond to the all-trans and 13-cis forms, respectively, according to the known linear correlation between ethylenic stretch frequencies and visible absorption maxima of retinal proteins (*31*). After illumination with a 515-nm laser for 1 h, the band at 1552 cm^{-1} disappeared. The remaining single peak at 1535 cm^{-1} in Figure 2 indicates a predominance of the all-trans form. Figure 2 also shows characteristic vibrational bands of the retinal skeleton, which will be referred to if they appear in the FTIR difference spectra described below.

Measurement of the NR_K Minus NR Difference Spectra. Figure 3a shows the NR_K minus NR difference spectrum measured at 77 K and pH 7. The ethylenic stretching vibration at 1536(−)/1526(+) cm^{-1} implies that NR is converted to a red-shifted intermediate, NR_K, upon light absorption at 77 K. There are negative bands at 1247, 1203, and 1166 cm^{-1} in the C−C stretching region and at 1010 cm^{-1} in the hydrogen out-of-plane (HOOP) region, which were also detected in the Raman spectrum (solid line of Figure 2). These spectral features are similar to those of BR (Figure 3b), suggesting that the NR to NR_K conversion is accompanied by the retinal photoisomerization from the all-trans to 13-cis form. Below, we compare the difference spectra measured for the two proteins, NR and BR, in detail.

Comparison of the Vibrational Bands of the Retinal Chromophore between NR and BR. Figure 4 compares the NR_K minus NR (a) and BR_K minus BR (b) spectra in the 1290−1130 cm^{-1} region. This frequency region includes the C−C stretching and the vinyl CCH rocking vibrations of the retinal chromophore. Negative bands in BR at 1255, 1216, 1203, and 1169 cm^{-1} are attributable to the C−C stretching vibrations of the retinal chromophore at the positions C12−C13, C8−C9, C14−C15, and C10−C11, respectively (Figure 4b) (*32*, *33*). The negative 1255 cm^{-1} band is composed of a mixture of D_2O-insensitive C12−C13 stretching and D_2O-sensitive lysine rocking vibrations (*34*, *35*). The positive 1194 cm^{-1} band of BR originates from C14−C15 and C10−C11 stretches (*36*). Analogous spectral features were observed for NR (Figure 4a), indicating similar chromophore conformation. We tentatively assigned the bands at 1247(−), 1215(−), 1203(−), and 1166(−) cm^{-1} as a mixture of the C12−C13 stretch and lysine rock, the C8−C9, C14−C15, and C10−C11 stretches, respectively. These bands were also observed at 1245, 1212, 1202, and 1166 cm^{-1} in the Raman spectrum measured upon hydration with H_2O (solid line of Figure 2), among which only the 1245 cm^{-1} band upshifted to 1258 cm^{-1} in D_2O (dotted line

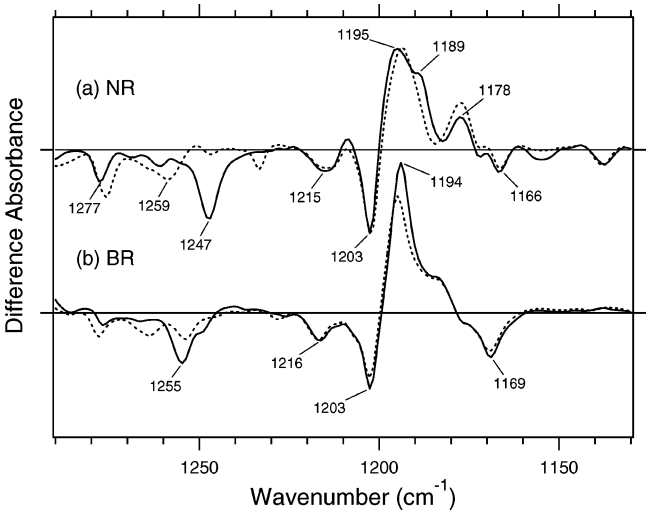

FIGURE 4: NR_K minus NR (a) and BR_K minus BR (b) spectra in the 1290−1130 cm^{-1} region, which correspond to C−C stretching vibrations and C−H and N−H in-plane rocking vibrations of the retinal chromophore. The sample was hydrated with H_2O (—) or D_2O (- - -). One division of the *y* axis corresponds to 0.004 absorbance units.

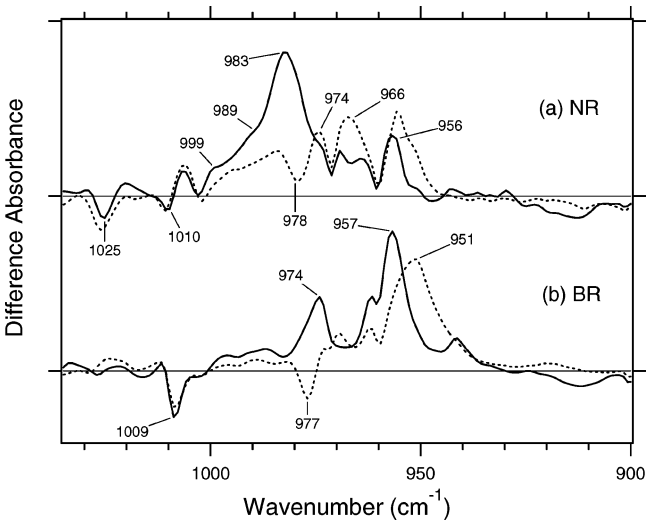

FIGURE 5: NR_K minus NR (a) and BR_K minus BR (b) spectra in the 1035−900 cm^{-1} region, which correspond to HOOP vibrations of the retinal chromophore. The sample was hydrated with H_2O (—) or D_2O (- - -). One division of the *y* axis corresponds to 0.0025 absorbance units.

of Figure 2). It seems that the Raman band at 1258 cm^{-1} corresponds to the C12−C13 stretching vibration in D_2O. The frequency of the C8−C9 and C14−C15 stretches in NR are almost identical to those in BR, while the C10−C11 and C12−C13 stretches are downshifted by 3 and 8 cm^{-1}, respectively, as also noted earlier (*19*). This result suggests that the chromophore structure of NR is somewhat different from that of BR in the middle of the retinal. The negative D_2O-insensitive peak at 1277 cm^{-1} in NR is prominent and also observed at 1274 cm^{-1} in the Raman spectra. In the case of BR, a similar Raman band at 1273 cm^{-1} was assigned as the C11−H in-plane rocking vibration (*35*). The observation of this band in the NR_K minus NR spectra suggests that structural changes of the chromophore at C11 upon photoisomerization are larger in NR than in BR.

Figure 5 shows the NR_K minus NR (a) and BR_K minus BR (b) spectra in the 1035−900 cm^{-1} region. It is well-known that the HOOP vibrations of the retinal chromophore appear in this region and that HOOP modes provide information on chromophore distortions (*32*, *37*−*40*). The D_2O/H_2O exchange-insensitive negative peak at 1009 cm^{-1} in Figure 5b was assigned as the symmetric in-plane methyl rocking combination involving mainly the methyl groups at C9 and C13 positions in BR (*35*). The 977 cm^{-1} band is observed for the D_2O-treated samples only and is assigned as the N−D in-plane rocking vibration downshifted from 1348 cm^{-1} upon hydration with D_2O. The appearance of a sharp peak at 957 cm^{-1} is characteristic for the BR_K minus BR spectrum, and the D_2O-sensitive bands at 974 and 957 cm^{-1} were assigned as HOOP vibrations of C15−H and N−H (*33*). This result indicates that the retinal distortions upon BR_K formation are localized in the Schiff base region. More complex spectral features were observed in the NR_K minus NR spectra, which look similar to those of *pp*R (*28*). The negative peak at 1010 cm^{-1} also appeared in the Raman spectra at 1011 cm^{-1} (Figure 2), which is assignable to the symmetric in-plane methyl rocking vibration. The 1025 cm^{-1} band was detected only in NR and may originate from protein vibrations, given its absence in the Raman spectra (Figure 2). The negative peak at 978 cm^{-1} in D_2O is probably obscured by large positive bands. The corresponding Raman band is at 979 cm^{-1} in D_2O (Figure 2), which is assignable to the N−D in-plane rocking vibration downshifted from 1337 cm^{-1} upon hydration with D_2O. As for the positive side, the bands at 999 and 983 cm^{-1} and the shoulder at 989 cm^{-1} are sensitive to D_2O. These bands are probably attributed to the HOOP vibrations of C15−H and/or N−H. The bands at 974, 966, and 956 cm^{-1} are insensitive to D_2O, possibly originating from other HOOP modes. An appearance of the D_2O-insensitive HOOP modes in NR is more similar to *pp*R than to BR, suggesting that specific distortions occur in the middle of the chromophore.

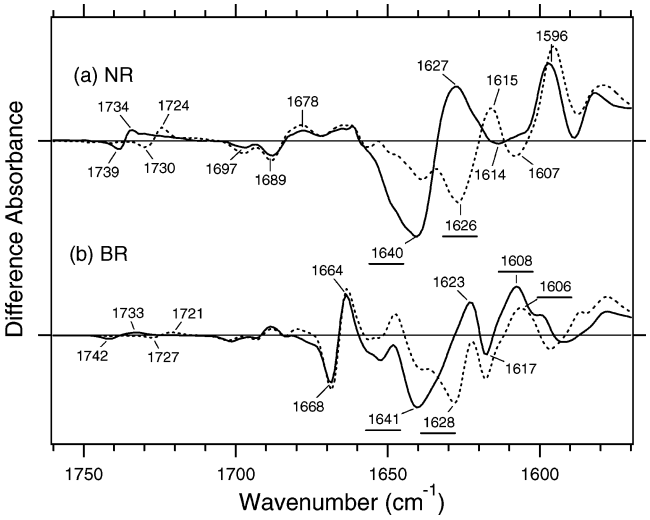

FIGURE 6: NR_K minus NR (a) and BR_K minus BR (b) spectra in the 1760−1570 cm^{-1} region, most of which are ascribable to vibrations of the protein moiety. The underlined peaks are C═N stretching vibrations of the chromophore. The sample was hydrated with H_2O (—) or D_2O (- - -). One division of the *y* axis corresponds to 0.004 absorbance units.

Figure 6 shows the NR_K minus NR (a) and the BR_K minus BR (b) spectra in the 1760−1570 cm^{-1} region, where most of the bands originate from vibrations of the protein. One exception is the C═N stretching vibration of the retinal Schiff

base that appears in the 1650−1600 cm^{-1} region. In BR, the C═N stretch has been observed at 1641 cm^{-1} in H_2O and at 1628 cm^{-1} in D_2O (Figure 6b) (*41*). This frequency upshift in H_2O is caused by coupling to the N−H bending vibration of the Schiff base, and the difference in frequency between H_2O and D_2O has been regarded as a measure of hydrogen-bonding strength of the Schiff base (*31*, *42*, *43*). The small difference in BR_K (1608 cm^{-1} in H_2O versus 1606 cm^{-1} in D_2O) has been interpreted in terms of the lack of a hydrogen bond for the Schiff base nitrogen after photoisomerization (*33*, *44*). In NR, the negative bands at 1640 and 1626 cm^{-1} are likely to originate from the C═N stretches in H_2O and D_2O, respectively (Figure 6a). These IR bands are in close frequency to the Raman bands at 1643 and 1625 cm^{-1} (Figure 2) because of the C═N stretches in H_2O and D_2O, respectively. The similarity in frequency shifts between NR and BR [14 versus 13 cm^{-1} in the presented FTIR spectra and 18 versus 17 cm^{-1} in the Raman spectra presented here and measured earlier (*45*)] implies the same hydrogen-bonding strength of the Schiff base in NR and BR. This is in contrast to the case of the positive 1627 and 1615 cm^{-1} bands, which are candidates for the C═N stretching mode of NR_K in H_2O and D_2O, respectively. If this assignment is correct, the greater H_2O/D_2O frequency difference in NR_K as compared to BR_K [12 versus 2 cm^{-1} in the presented FTIR spectra] may indicate that the hydrogen bond of the Schiff base in NR_K is not disrupted after photoisomerization, unlike that in BR. There is another possibility that the 1596 cm^{-1} band is the C═N stretch of the Schiff base, where the deuterium shift is as small as that of BR. To distinguish between the two possibilities, we measured the N−D stretching vibration of the Schiff base to monitor its hydrogen-bonding strength directly, which is shown below.

Comparison of the Vibrational Bands of the Protein Moiety between NR and BR. The bands in Figure 6 (except the C═N stretching vibrations of the Schiff base) come from the protein moieties of NR and BR. In BR, the 1742(−)/1733(+) cm^{-1} bands in H_2O are shifted to 1727(−)/1721(+) cm^{-1} in D_2O, which was previously assigned as the C═O stretch of Asp115 (*46*) (the homologous residue in NR is Asp161 in helix D). Because the similar spectral changes are observed at 1739(−)/1734(+) cm^{-1} in H_2O and 1730(−)/1724(+) cm^{-1} in D_2O for NR (Figure 6a), these bands can be assigned to the C═O stretch of Asp161. As in BR, the aspartic acid at this position is protonated in NR, and the hydrogen-bonding alterations upon retinal isomerization are similar.

The bands at 1623(+)/1617(−) cm^{-1} in Figure 6b were previously assigned as the C═O stretch of the peptide carbonyl (amide I vibration) of Val49 (*47*) near the Schiff base of BR. The bands at 1668(−)/1664(+) cm^{-1} are highly dichroic (*30*) and appear in the typical frequency region of the amide I vibration of the α_{II} helix (*48*), which is probably located in the transmembrane region. In NR, the spectral changes caused by the amide I vibrations of α_{II} helix are very small, while there are several bands in higher and lower frequency regions. The bands at 1697(−), 1689(−) and 1678(+) cm^{-1} are assignable to the C═O stretches of the peptide carbonyls with very weak hydrogen bonds. The 1596 cm^{-1} band, which is relatively large, is not observed in BR_K in this frequency region; the corresponding negative band may be located at 1607 cm^{-1}. The frequencies of these

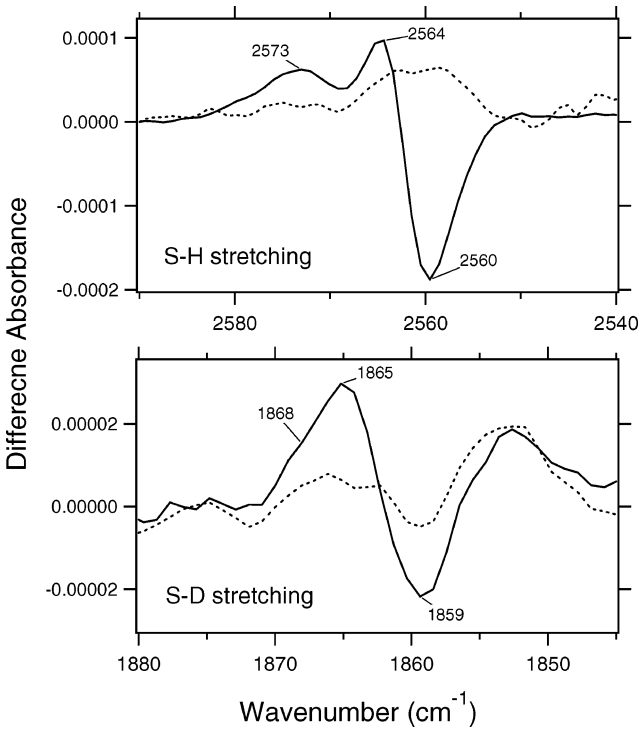

FIGURE 7: NR_K minus NR spectra in the 2590−2540 cm^{-1} (upper panel) and 1880−1845 cm^{-1} (lower panel) region, which correspond to S−H and S−D stretching vibrations of cysteine residues, respectively. The sample was hydrated with H_2O (— in the upper panel and - - - in the lower panel) or D_2O (- - - lines in the upper panel and — in the lower panel). The spectra were recorded at 100 K to improve the signal-to-noise ratio in these frequency regions. One division of the *y* axis corresponds to 0.0001 (upper panel) or 0.000 02 (lower panel) absorbance units.

bands are too low to originate from the C═O stretching vibrations of peptide carbonyls. As described above, the possibility that these bands belong to the C═N stretch cannot be excluded at this moment. A similar large band was also observed in the *p*pR_K minus *p*pR spectrum (*28*).

Structural Changes of Cysteine Residues upon the Retinal Isomerization. Figure 7 shows the NR_K minus NR spectra in the 2590−2540 cm^{-1} (the upper panel) and 1880−1845 cm^{-1} (the lower panel) regions, which correspond to S−H and S−D stretching vibrations of cysteine residues, respectively. These spectra were recorded at 100 K to increase the signal-to-noise ratio. We confirmed that the same vibrational bands are observed at 77 K also but with reduced intensity (data not shown). There is one negative peak at 2560 cm^{-1} and two positive peaks at 2573 and 2564 cm^{-1} in the S−H stretching region. These bands completely downshift to 1859(−) and to 1868(+) and 1865(+) cm^{-1} in the S−D stretching region, respectively. The bands at 2560(−)/2564(+) cm^{-1} were also reported by Bergo et al. in the infrared difference spectra measured at 253 K (*20*). Because their spectra report on the late photocycle intermediates, the observed frequency change of the S−H group is persistent over a wide time range. Another band at 2573 cm^{-1} may originate from heterogeneity of the environment around the S−H group in NR_K. The fact that the frequency changes of the S−H groups occur as early as NR_K suggest that the cysteine is located close to the retinal. Cys167 and especially Cys190, which are located around the β-ionone ring of the retinal, are good candidates for those spectral features.

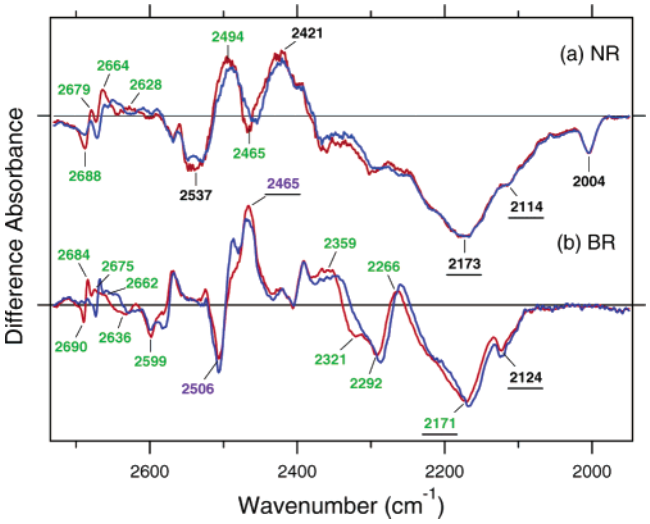

FIGURE 8: Comparison of the difference IR spectra of the samples hydrated with D_2O (red lines) and $D_2{}^{18}O$ (blue lines) in the 2730−1950 cm^{-1} region. The spectra were recorded at 100 K to improve the signal-to-noise ratio in this frequency region. Green-labeled frequencies correspond to those identified as water stretching vibrations. Purple-labeled frequencies are O−D stretches of Thr89 (*60*, *61*), while the underlined frequencies are N−D stretches of the Schiff base (*62*). The spectrum in (b) is reproduced from Tanimoto et al. (*24*), where the sample window is tilted by 53.5°. One division of the *y* axis corresponds to 0.0006 absorbance units. The distortion around the 2300 cm^{-1} region was caused by variation in the CO_2 concentration during the measurement.

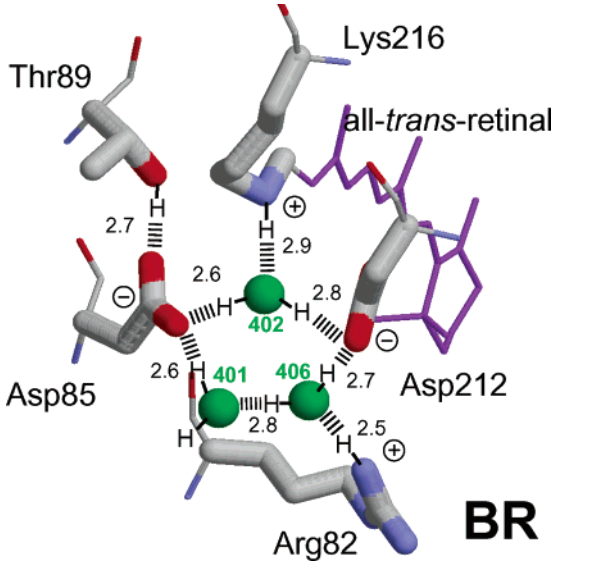

FIGURE 9: X-ray crystallographic structures of the Schiff base region of BR from PDB entry 1C3W (*54*). Top and bottom regions correspond to the cytoplasmic and extracellular sides, respectively, with the membrane normal being approximately vertical. Green spheres (waters 401, 402, and 406) represent water molecules that form a roughly pentagonal cluster with an oxygen from Asp85 and an oxygen from Asp212. The pentagonal cluster structure will stabilize an electric quadrupole in this region. Hydrogen atoms and hydrogen bonds (- - -) are deduced from the structure; the numbers are the hydrogen-bond distances in angstroms.

Comparison of the Structure of the Schiff Base Region between NR and BR. Figure 8 shows the NR_K minus NR (a) and the BR_K minus BR (b) spectra in the 2730−1970 cm^{-1} region, which contains the X−D stretching vibrations of protein and water molecules. A spectral comparison between the samples hydrated with D_2O and $D_2{}^{18}O$ reveals O−D stretching vibrations of water molecules, which change its frequencies upon retinal photoisomerization. The vibrational bands exhibiting isotope-induced downshifts are assignable to the O−D stretching vibrations of water (labeled in green, Figure 8). The NR_K minus NR spectra were recorded at 100 K to increase the signal-to-noise ratio. We also confirmed that the same vibrational bands are observed in the spectra recorded at 77 K, but with reduced intensity (data not shown). In BR, six negative peaks at 2690, 2636, 2599, 2321, 2292, and 2171 cm^{-1} were earlier assigned to vibrations of water molecules. The bands are widely distributed over the possible frequency range for stretching vibrations of water (Figure 8b). Because the frequencies of the negative peaks at 2321, 2292, and 2171 cm^{-1} are much lower than those of fully hydrated tetrahedral water molecules (*49*−*51*), the hydrogen bonds of those water molecules must be very strong, possibly indicating their association with negative charges. Indeed, we recently assigned the 2171 cm^{-1} band to the O−D group of a water molecule associated with deprotonated Asp85 (*52*). This water molecule, called 402 in the crystal structure of BR (PDB entry 1C3W), is located between the Schiff base and Asp85 (see also Figure 9). A previous QM/MM calculation of the Schiff base region of BR also supported the existence of an extremely strong hydrogen bond between water 402 and Asp85 (*53*). Water stretching vibrations of BR_K tend to be higher in frequency, implying that the overall hydrogen bonding becomes weaker upon photoisomerization.

Interestingly, in NR, only two negative peaks assignable to the O−D stretching vibrations of water at 2688 and 2465 cm^{-1} were observed. The water stretching vibrations of NR_K were assigned to the bands at 2679, 2664, 2628, and 2494 cm^{-1}. It should be emphasized that there are no water bands in the <2400 cm^{-1} region in a significant contrast to the reported cases of archaeal rhodopsins such as BR and *pp*R. In the case of *pp*R, two pairs of peaks were observed in the <2400 cm^{-1} region, located at 2369(+)/2307(−) and 2274(+)/2215(−) cm^{-1} (*29*). There are several possible explanations for the lack of bands of water under strong hydrogen-bonding conditions in NR: (i) NR lacks water molecules in the Schiff base region; (ii) NR possesses water molecules in the Schiff base region, but their O−D vibrations are located at the higher frequency side (>2400 cm^{-1}); and (iii) NR possesses water molecules in the Schiff base region with O−D stretches at <2400 cm^{-1}, but there are no frequency changes upon retinal isomerization.

As shown in Figure 9, the BR structure possesses a water-containing pentagonal cluster in the Schiff base region (*54*, *55*). This is the case not only for BR, but also for *pp*R (*56*, *57*) and HR (*58*), the latter having one of the aspartates replaced by a chloride ion. In all archaeal rhodopsins with known structures, three water molecules are present in the Schiff base region, possibly hydrating the charged groups. Because many of the key amino acids are conserved in the Schiff base region between NR and BR, such as Arg128, Asp131, Trp132, Thr135, Trp230, Tyr233, Pro234, Asp259, Ala262, and Lys263 in NR (Arg82, Asp85, Trp86, Thr89, Trp182, Tyr185, Pro186, Asp212, Ala215, and Lys216, respectively, in BR), it is reasonable to assume that NR also possesses the water-containing pentagonal cluster.

It was found earlier that NR does not pump protons, even though the amino acids constituting the proton-conducting

pathway in BR are almost completely conserved and the retinal configuration in NR is very much BR-like as evidenced by Raman spectra (*19*). It was suggested that NR may not transport protons despite all of the structural similarities with BR because its reprotonation switch is not functional. Absence of water bands in the <2400 cm^{-1} region in NR may be correlated with this fact, keeping in mind that the BR mutants (D85N and D212N) lacking water bands at <2400 cm^{-1} do not pump protons in the absence of a Cl^- ion (*59*). On the other hand, protons are pumped by various BR mutants if strong hydrogen-bonded water molecules (<2400 cm^{-1}) are present, such as T89A, Y185F (*52*), T46V, R82Q, D96N, D115N, and E204Q (Shibata and Kandori, unpublished). Thus, the strong hydrogen-bonded water molecules may be functionally important. The underlying molecular mechanism is still an open question, but one can state that the rearrangement of a water-containing hydrogen-bonded network must be correlated with the reprotonation switch.

The frequency region shown in Figure 8 also contains X−D stretching vibrations other than those of water molecules. In the BR_K minus BR spectrum, the bands at 2506(−)/2465(+) cm^{-1} labeled in a purple color and the underlined bands at 2465(+), 2171(−) and 2124(−) cm^{-1} were assigned to the O−D stretching vibrations of Thr89 (*60*, *61*) and the N−D stretching vibrations of the retinal Schiff base (*62*), respectively. Thus, the negative 2171 cm^{-1} band contains both the O−D stretch of water and the N−D stretch of the Schiff base. In the NR_K minus NR spectrum, there are five bands at 2537(−), 2421(+), 2173(−), 2114(−), and 2004(−) cm^{-1}, which do not originate from water vibrations. The bands at 2537(−)/2494(+) cm^{-1} are assignable to the O−D stretching vibrations of Thr135 using analogy with BR. The peak at 2494 cm^{-1} probably contains the O−D stretching vibrations of both water and Thr135, which can be inferred from its amplitude being larger than that of the corresponding negative band at 2465 cm^{-1}. The O−D frequency of Thr135 in NR (2537 cm^{-1}), which is higher than that of Thr89 in BR (2506 cm^{-1}), indicates that the hydrogen-bonding strength between Thr135 and Asp131 is weaker than that between Thr89 and Asp85 in BR.

Though not assigned directly by use of the labeled protein, the bands at 2173 and 2114 cm^{-1} are likely to originate from N−D stretching of the Schiff base, whose frequencies are almost identical to those in BR (2171 and 2124 cm^{-1}). This indicates identical hydrogen-bonding strengths between NR and BR, which are consistent with the results obtained for the C═N stretching vibrations shown above (Figure 6). In contrast, the analysis of the C═N stretching vibrations of NR_K suggested a very different hydrogen-bonding strength of the Schiff base than the one inferred from the N−D stretches shown in Figure 8. Clear presence of the BR-like negative bands at 2173 and 2114 cm^{-1} strongly suggests that the N−D stretch is upshifted in NR_K, indicating its weakened hydrogen bond. We consider the 2421 cm^{-1} band to be the most likely candidate for the N−D stretch in NR_K. In this case, the hydrogen-bonding alterations of the protonated Schiff base are essentially identical between NR and BR, where the hydrogen bond is disrupted upon retinal isomerization. The lower frequency observed for NR_K (2421 cm^{-1} versus 2465 cm^{-1} in BR_K) suggests a somewhat stronger hydrogen bond of the Schiff base of NR after isomerization.

The negative band located at 2004 cm^{-1} in NR hydrated with D_2O (Figure 8a) was observed at 2617 cm^{-1} in the NR_K minus NR spectrum in H_2O (data not shown). This band is not detected in BR as shown in Figure 8b, but a smaller and broader band exists at 2003 cm^{-1} on the negative side of the *p*R_K minus *p*R spectrum (*29*). This band may originate from the N−D stretching vibration with an extremely strong hydrogen bond. The corresponding band in NR_K is not seen on the positive side of the spectrum, or surprisingly, its frequency may have changed to 2421 or 2494 cm^{-1}, which correspond to N−D stretching vibrations with weak hydrogen bonds.

DISCUSSION

In this paper, we investigated NR expressed in *P. pastoris* by Raman and low-temperature FTIR spectroscopy. NR is the first archaeal rhodopsin-like protein discovered in eucaryotes (*16*). Sequence alignment analysis suggests that NR has a structure similar to those of archaeal rhodopsins. In fact, only 6 of 25 amino acids constituting the retinal binding pocket are different from those of BR (Figure 1), while 10 amino acids are different in *p*pR. Because of the particular sequence similarity with BR, NR was expected to work as a proton pump. However, the previous study showed that NR lacks proton-pumping activity (*19*). In addition, earlier flash-photolysis and time-resolved FTIR studies found that its photocycle is much slower than that of BR, and the decay times of the M and O intermediates were similar to those in *p*pR (*18*, *19*). These functional and photochemical differences between NR and BR must be correlated with their protein structures and light-induced structural changes. We thereby investigated them by means of vibrational spectroscopy.

Light Adaptation of NR. In the present study, we found that the dark-adapted NR sample possesses a significant amount of 13-*cis*-retinal in DMPC/DMPA liposomes. This is in clear contrast to NR in *P. pastoris* membranes, where the reconstitution with all-*trans*-retinal led to formation of only a small fraction of 13-*cis*-retinal as shown by subsequent extraction of retinal (*18*). In the previous paper (*19*), both dehydration and treatment with detergents increased the amount of the 13-*cis*-retinal as in the case of BR. These facts suggest the important role of the surrounding lipids and water in a thermal equilibrium between 13-cis and all-trans forms. Further experiments will be needed to elucidate the biological significance of the light adaptation of NR.

Presence of the 13-cis form often makes it difficult to do a thorough spectroscopic analysis of archaeal rhodopsins. Because no light-adaptation procedure has been reported for NR so far, we established it for the NR samples in the DMPC/DMPA liposomes. The illumination regime is similar to that for BR, although the illumination times are completely different. In the case of BR, illumination for 2 min is sufficient to entirely convert the 13-cis form to all-trans under the present experimental conditions, where temperature is kept at 273 K to prevent thermal reversion from the all-trans to 13-cis form. In contrast, much longer illumination is required for NR under the same experimental conditions, consequently, we illuminated the NR sample for 1 h at room temperature. The thermal reversion was also very slow, so that we were able to rehydrate the all-trans NR sample for the FTIR measurements after light adaptation. It is likely

that these unique properties of NR are correlated with the structure of the retinal-binding pocket, including the internal water molecules.

Chromophore Structure and Its Interaction with Protein in NR and BR. The spectral comparison of the C−C stretching vibrations of the retinal chromophore (Figures 2 and 4) revealed that the conformation of the polyene chain in NR is similar to that in BR. Because BR has a planar polyene chain (*54*, *55*), this is likely to be the case for NR as well. In general, these spectral features are also shared by *p*pR. However, the lower frequencies of the C12−C13 and C10−C11 stretching vibrations in NR suggest that its chromophore structure in the middle of the polyene chain is somewhat different from that of BR and *p*pR. The difference between C═NH and C═ND stretching vibrations and the frequency of N−D stretching vibration of the retinal Schiff base are regarded as markers of its hydrogen-bonding strength. The values of the former in NR and BR are 14 and 13 cm^{-1} in the presented FTIR spectra and 18 and 17 cm^{-1} in the Raman spectra presented here and measured earlier, respectively. The N−D stretching frequencies of the Schiff base are 2173 cm^{-1} in NR and 2171 cm^{-1} in BR. These are similar to each other and suggest that the hydrogen-bonding strength of the Schiff base is almost the same as that in NR and BR. This is in clear contrast to *p*pR, which has a very strong hydrogen-bonded Schiff base. This difference may be caused by the four additional amino acid replacements in its retinal-binding site (Leu139 to Ile, Asp161 to Asn, Met164 to Val, and Ala262 to Thr in *p*pR, using the NR numbering). For these reasons, we assume that the retinal structure of NR is very similar to that of BR as predicted from the sequence similarity in the retinal-binding site.

Although the structure of retinal in NR is similar to that in BR, the structural changes upon photoisomerization are quite different. The most obvious differences were observed in the HOOP region. The larger number of HOOP bands in NR_K implies that the structural changes of retinal extend from the Schiff base region to the polyene chain, similarly to the case of *p*pR. The observation of the light-induced changes in S−H stretching vibrations may also support the notion of the extended structural changes of the retinal, because cysteine residues are not found in the Schiff base region of NR as judged from the X-ray crystal structure of BR (*54*, *55*). One of the most significant differences between NR and BR can be seen in the amide-I vibrations. In the case of BR, the presence of the bands at 1668(−)/1664(+) cm^{-1} demonstrates the local perturbation of the peptide backbone in an α_{II} helix (*48*), which is probably located in a transmembrane region (Figure 6b). In contrast, no spectral changes in the amide-I vibrations associated with helical regions (1670−1650 cm^{-1}) were detected for NR (Figure 6a). This fact may suggest that the chromophore−protein coupling is weaker in NR than in BR.

Pentagonal Cluster Structure Containing Water Molecules in NR. Figure 9 shows the pentagonal cluster structure around the Schiff base region of BR. Many vibrational modes originating from this region appeared in the BR_K minus BR spectra. In particular, we found the O−D stretching vibrations in the extraordinary low-frequency region (*49*) and assigned one of them to the O−D group of water 402, which hydrates Asp85 (*52*). Interestingly, only two negative peaks at 2688 and 2645 cm^{-1} coresponding to the O−D stretching vibrations of water were observed in NR (Figure 8). It should be particularly emphasized that there are no water bands in the <2400 cm^{-1} region, which is in prominent contrast to the reported archaeal rhodopsins such as BR and *p*pR. As discussed in the Results, there are three possibilities for the lack of water bands under strong hydrogen-bonding conditions in NR: (i) NR lacks water molecules in the Schiff base region; (ii) O−D stretches of the water molecules in the Schiff base region are located at >2400 cm^{-1}; and (iii) O−D stretches of the water molecules in the Schiff base region at <2400 cm^{-1} exhibit no frequency changes upon retinal isomerization.

Although we cannot exclude any of the three possibilities at this time, the first possibility is the least plausible. Because of the high similarity of the amino acid sequences of NR and BR, it is reasonable to expect that NR possesses a water-containing pentagonal cluster in the Schiff base region similar to that of BR (Figure 9). A similar hydrogen-bonding strength of the protonated Schiff base in NR and BR strongly supports this hypothesis, as the hydrogen-bond acceptor of the Schiff base in BR is a water molecule. If the 2537 cm^{-1} band originates from the O−D stretch of Thr135 in NR, its hydrogen bond is also similar to that of Thr89 in BR, though it is slightly weaker. If NR possesses the water-containing pentagonal-cluster structure like those of BR and *p*pR, the observed lack of strong hydrogen-bonded waters could be explained by either weak interaction of the water [case (ii)] or the absence of light-induced hydrogen-bond alterations [case (iii)]. In the former case, a weak hydrogen bond of the bridging water with the negatively charged Asp131 may require another specific interaction to the water. Otherwise, interaction of the water with Asp131, as is the case of Asp85 in BR (*52*), should be strong, so that its O−D stretch is located at the low-frequency side (<2400 cm^{-1}). Because the retinal isomerization is likely to perturb the hydrogen-bonded network, hydrogen bonds of the water molecule(s) should be altered, as expected from the earlier observations for BR (*24*, *49*, *52*) and *p*pR (*29*). Thus, further experimental efforts are required to elucidate the structure of the hydrogen-bonded network in the Schiff base region of NR. At least, we can conclude that hydrogen bonds of internal water molecules are clearly different in NR versus BR and *p*pR.

The different hydrogen-bonding pattern of water molecules may be responsible for the fact that NR does not pump protons. The amino acids constituting the proton conducting pathway in BR are almost completely conserved in NR, and the retinal configuration is very BR-like in NR as evidenced by the Raman spectra (*19*). Nevertheless, why does NR not pump protons? The hypothesis is that NR may not transport protons despite all of the structural similarities with BR because its reprotonation switch is not functional. The latest views on the reprotonation switch mechanism of BR supported by X-ray diffraction data and FTIR spectroscopy stress the importance of strain in the retinal bonds and the interaction of its Schiff base with internal water molecules (*24*, *25*). The unique character of the hydrogen bonds of internal water molecules may provide a hint on the lack of the reprotonation switch in NR. Structural analysis of the late photointermediates will lead to a better understanding of this putative mechanism, which is our future focus.

ACKNOWLEDGMENT

We want to thank Elena and John Spudich for giving us the NR expression system and providing the training on its use. We thank Mikihiro Shibata for valuable discussions on the internal water molecules of BR. We also want to thank Jacek Lipkowski for letting us use the Raman spectrometer.

REFERENCES

1. Spudich, J. L., Yang, C., Jung, K., and Spudich, E. N. (2000) Retinylidene proteins: Structures and functions from archaea to humans, *Annu. Rev. Cell Dev. Biol. 16*, 365−392.
2. Jung, K. H., and Spudich, J. L. (2004) Microbial rhodopsins: Transport and sensory proteins throughout the three domains of life, in *CRC Handbook of Organic Photochemistry and Photobiology* (Horspool, W. M., and Lenci, F., Eds.) 2nd ed., section II photobiology, pp 124/1−124/11, CRC Press, Boca Raton, FL.
3. Nagel, G., Ollig, D., Fuhrmann, M., Kateriya, S., Musti, A. M., Bamberg, E., and Hegemann, P. (2002) Channelrhodopsin-1: A light-gated proton channel in green algae, *Science 296*, 2395−2398.
4. Sineshchekov, O. A., Jung, K.-H., and Spudich, J. L. (2002) Two rhodopsins mediate phototaxis to low- and high-intensity light in *Chlamydomonas reinhardtii*, *Proc. Natl. Acad. Sci. U.S.A. 99*, 8689−8694.
5. Ng, W. V., Kennedy, S. P., Mahairas, G. G., Berquist, B., Pan, M., Shukla, H. D., Lasky, S. R., Baliga, N. S., Thorsson, V., Sbrogna, J., Swartzell, S., Weir, D., Hall, J., Dahl, T. A., Welti, R., Goo, Y. A., Leithauser, B., Keller, K., Cruz, R., Danson, M. J., Hough, D. W., and Maddocks, D. (2000) Genome sequence of *Halobacterium* species NRC-1, *Proc. Natl. Acad. Sci. U.S.A. 97*, 12176−12181.
6. Lanyi, J. K. (1997) Mechanism of ion transport across membranes, *J. Biol. Chem. 272*, 31209−31212.
7. Haupts, U., Tittor, J., and Oesterhelt, D. (1999) Closing in on bacteriorhodopsin: Progress in understanding the molecule, *Annu. Rev. Biophys. Biomol. Struct. 28*, 367−399.
8. Lanyi, J. K. (1990) Halorhodopsin, a light-driven electrogenic chloride-transport system, *Physiol. Rev. 70*, 319−330.
9. Hoff, W. D., Jung, K. H., and Spudich, J. L. (1997) Molecular mechanism of photosignaling by archaeal sensory rhodopsins, *Annu. Rev. Biophys. Biomol. Struct. 26*, 223−258.
10. Kamo, N., Shimono, K., Iwamoto, M., and Sudo, Y. (2001) Photochemistry and photoinduced proton-transfer by *pharaonis* phoborhodopsin, *Biochemistry (Moscow) 66*, 1277−1282.
11. Sasaki, J., and Spudich, J. L. (2000) Proton transport by sensory rhodopsins and its modulation by transducer-binding, *Biochim. Biophys. Acta 1460*, 230−239.
12. Brown, L. S. (2004) Fungal rhodopsins and opsin-related proteins: Eukaryotic homologues of bacteriorhodopsin with unknown functions, *Photochem. Photobiol. Sci. 3*, 555−565.
13. Beja, O., Aravind, L., Koonin, E. V., Suzuki, M. T., Hadd, A., Nguyen, L. P., Jovanovich, S. B., Gates, C. M., Feldman, R. A., Spudich, J. L., Spudich, E. N., and DeLong, E. F. (2000) Bacterial rhodopsin: Evidence for a new type of phototrophy in the sea, *Science 289*, 1902−1906.
14. de la Torre, J. R., Christianson, L. M., Beja, O., Suzuki, M. T., Karl, D. M., Heidelberg, J., and DeLong, E. F. (2003) Proteorhodopsin genes are distributed among divergent marine bacterial taxa, *Proc. Natl. Acad. Sci. U.S.A. 100*, 12830−12835.
15. Jung, K. H., Trivedi, V. D., and Spudich, J. L. (2003) Demonstration of a sensory rhodopsin in eubacteria, *Mol. Microbiol. 47*, 1513−1522.
16. Bieszke, J. A., Braun, E. L., Bean, L. E., Kang, S., Natvig, D. O., and Borkovich, K. A. (1999) The nop-1 gene of *Neurospora crassa* encodes a seven transmembrane helix retinal-binding protein homologous to archaeal rhodopsins, *Proc. Natl. Acad. Sci. U.S.A. 96*, 8034−8039.
17. Okamoto, O. K., and Hastings, J. W. (2003) Novel dinoflagellate clock-related genes identified through microarray analysis, *J. Phycol. 39*, 519−526.
18. Bieszke, J. A., Spudich, E. N., Scott, K. L., Borkovich, K. A., and Spudich, J. L. (1999) A eukaryotic protein, NOP-1, binds retinal to form an archaeal rhodopsin-like photochemically reactive pigment, *Biochemistry 38*, 14138−14145.
19. Brown, L. S., Dioumaev, A. K., Lanyi, J. K., Spudich, E. N., and Spudich, J. L. (2001) Photochemical reaction cycle and proton transfers in *Neurospora* rhodopsin, *J. Biol. Chem. 276*, 32495−32505.
20. Bergo, V., Spudich, E. N., Spudich, J. L., and Rothschild, K. J. (2002) A Fourier transform infrared study of *Neurospora* rhodopsin: Similarities with archaeal rhodopsins, *Photochem. Photobiol. 76*, 341−349.
21. Idnurm, A., and Howlett, B. J. (2001) Characterization of an opsin gene from the ascomycete *Leptosphaeria maculans*, *Genome 44*, 167−171.
22. Dawe, A. L., McMains, V. C., Panglao, M., Kasahara, S., Chen, B., and Nuss, D. L. (2003) An ordered collection of expressed sequences from *Cryphonectria parasitica* and evidence of genomic microsynteny with *Neurospora crassa* and *Magnaporthe grisea*, *Microbiology 149*, 2373−2384.
23. Keon, J., Bailey, A., and Hargreaves, J. (2000) A group of expressed cDNA sequences from the wheat fungal leaf blotch pathogen, *Mycosphaerella graminicola* (*Septoria tritici*), *Fungal Genet. Biol. 29*, 118−133.
24. Tanimoto, T., Furutani, Y., and Kandori, H. (2003) Structural changes of water in the Schiff base region of bacteriorhodopsin: Proposal of a hydration switch model, *Biochemistry 42*, 2300−2306.
25. Lanyi, J. K., and Schobert, B. (2004) Local-global conformational coupling in a heptahelical membrane protein: Transport mechanism from crystal structures of the nine states in the bacteriorhodopsin photocycle, *Biochemistry 43*, 3−8.
26. Kates, M., Kushwaha, S. C., and Sprott, G. D. (1982) Lipids of purple membrane from extreme halophiles and of methanogenic bacteria, *Methods Enzymol. 88*, 98−111.
27. Pitard, B., Richard, P., Duñach, M., Girault, G., and Rigaud, J.-L. (1996) ATP synthesis by the F_OF_1ATP synthase from thermophilic *Bacillus* PS3 reconstituted into liposomes with bacteriorhodopsin. 1. Factors defining the optimal reconstitution of ATP synthases with bacteriorhodopsin, *Eur. J. Biochem. 235*, 769−778.
28. Kandori, H., Shimono, K., Sudo, Y., Iwamoto, M., Shichida, Y., and Kamo, N. (2001) Structural changes of *pharaonis* phoborhodopsin upon photoisomerization of the retinal chromophore: Infrared spectral comparison with bacteriorhodopsin, *Biochemistry 40*, 9238−9246.
29. Kandori, H., Furutani, Y., Shimono, K., Shichida, Y., and Kamo, N. (2001) Internal water molecules of *pharaonis* phoborhodopsin studied by low-temperature infrared spectroscopy, *Biochemistry 40*, 15693−15698.
30. Kandori, H., Kinoshita, N., Shichida, Y., and Maeda, A. (1998) Protein structural changes in bacteriorhodopsin upon photoisomerization as revealed by polarized FTIR spectroscopy, *J. Phys. Chem. B 102*, 7899−7905.
31. Aton, B., Doukas, A. G., Callender, R. H., Becher, B. and Ebrey, T. G. (1977) Resonance Raman studies of the purple membrane, *Biochemistry 16*, 2995−2999.
32. Maeda, A. (1995) Application of FTIR spectroscopy to the structural study on the function of bacteriorhodopsin, *Isr. J. Chem. 35*, 387−400.
33. Smith, S. O., Lugtenburg, J., and Mathies, R. A. (1985) Determination of retinal chromophore structure in bacteriorhodopsin with resonance Raman spectroscopy, *J. Membr. Biol. 85*, 95−109.
34. Maeda, A., Sasaki, J., Pfefferlé, J.-M., Shichida, Y., and Yoshizawa, T. (1991) Fourier transform infrared spectral studies on the Schiff base mode of all-*trans* bacteriorhodopsin and its photointermediates, K and L, *Photochem. Photobiol. 54*, 911−921.
35. Smith, S. O., Braiman, M. S., Myers, A. B., Pardoen, J. A., Courtin, J. M. L., Winkel, C., Lugtenburg, J., and Mathies, R. A. (1987) Vibrational analysis of the all-*trans*-retinal chromophore in light-adapted bacteriorhodopsin, *J. Am. Chem. Soc. 109*, 3108−3125.
36. Gerwert, K., and Siebert, F. (1986) Evidence for light-induced 13-cis, 14-s-cis isomerization in bacteriorhodopsin obtained by FTIR difference spectroscopy using isotopically labeled retinals, *EMBO J. 5*, 805−811.
37. Mathies, R. A., Lin, S. W., Ames, J. B., and Pollard, W. T. (1991) From femtoseconds to biology: Mechanism of bacteriorhodopsin's light-driven proton pump, *Annu. Rev. Biophys. Biophys. Chem. 20*, 491−518.
38. Rothschild, K. J. (1992) FTIR difference spectroscopy of bacteriorhodopsin: Toward a molecular model, *J. Bioenerg. Biomembr. 24*, 147−167.

39. Siebert, F. (1995) Infrared spectroscopy applied to biochemical and biological problems, *Methods Enzymol. 246*, 501−526.
40. Gerwert, K. (1999) Molecular reaction mechanisms of proteins monitored by time-resolved FTIR-spectroscopy, *Biol. Chem. 380*, 931−935.
41. Siebert, F., and Mäntele, W. (1983) Investigation of the primary photochemistry of bacteriorhodopsin by low-temperature Fourier-transform infrared spectroscopy, *Eur. J. Biochem. 130*, 565−573.
42. Rodman-Gilson, H. S., Honig, B., Croteau, A., Zarrilli, G., and Nakanishi, K. (1988) Analysis of the factors that influence the C═N stretching frequency of polyene Schiff bases. Implications for bacteriorhodopsin and rhodopsin, *Biophys. J. 53*, 261−269.
43. Baasov, T., Friedman, N., and Sheves, M. (1987) Factors affecting the C═N stretching in protonated retinal Schiff base: A model study for bacteriorhodspsin and visual pigments, *Biochemistry 26*, 3210−3217.
44. Rothschild, K. J., Roepe, P., Lugtenburg, J., and Pardoen, J. A. (1984) Fourier transform infrared evidence for Schiff base alteration in the first step of the bacteriorhodopsin photocycle, *Biochemistry 23*, 6103−6109.
45. Diller, R., Stockburger, M., Oesterhelt, D., and Tittor, J. (1987) Resonance Raman study of intermediates of the halorhodopsin photocycle, *FEBS Lett. 217*, 297−304.
46. Braiman, M. S., Mogi, T., Marti, T., Stern, L. J., Khorana, H. G., and Rothschild, K. J. (1988) Vibrational spectroscopy of bacteriorhodopsin mutants: Light-driven proton transport involves protonation changes of aspartic acid residues 85, 96, and 212, *Biochemistry 27*, 8516−8520.
47. Yamazaki, Y., Tuzi, S., Saitô, H., Kandori, H., Needleman, R., Lanyi, J. K., and Maeda, A. (1996) Hydrogen bonds of water and C═O groups coordinate long-range structural changes in the L photointermediate of bacteriorhodopsin, *Biochemistry 35*, 4063−4068.
48. Krimm, S., and Dwivedi, A. M. (1982) Infrared spectrum of the purple membrane: Clue to a proton conduction mechanism? *Science 216*, 407−408
49. Kandori, H., and Shichida, Y. (2000) Direct obserbation of the bridged water stretching vibrations inside a protein, *J. Am. Chem. Soc. 122*, 11745−11746.
50. Monosmith, W. B., and Walrafen, G. E. (1984) Temperature dependence of the Raman hydroxyl-stretching overtone from liquid water, *J. Chem. Phys. 81*, 669−674.
51. Walrafen, G. E., and Fisher, M. R. (1986) Low-frequency Raman scattering from water and aqueous solutions: A direct measure of hydrogen-bonding, *Methods Enzymol. 127*, 91−105.
52. Shibata, M., Tanimoto, T., and Kandori, H. (2003) Water molecules in the Schiff base region of bacteriorhodopsin, *J. Am. Chem. Soc. 125*, 13312−13313.
53. Hayashi, S., and Ohmine, I. (2000) Proton transfer in bacteriorhodopsin: Structure, excitation, IR spectra, and potential energy surface analyses by an *ab initio* QM/MM method, *J. Phys. Chem. B 104*, 10678−10691.
54. Luecke, H., Schobert, B., Richter, H.-T., Cartailler, J. P., and Lanyi, J. K. (1999) Structure of bacteriorhodopsin at 1.55 Å resolution, *J. Mol. Biol. 291*, 899−911.
55. Belrhali, H., Nollert, P., Royant, A., Menzel, C., Rosenbusch, J. P., Landau, E. M., and Pebay-Peyroula, E. (1999) Protein, lipid, and water organization in bacteriorhodopsin crystals: A molecular view of the purple membrane at 1.9 Å resolution, *Structure 15*, 909−917.
56. Luecke, H., Schobert, B., Lanyi, J. K., Spudich, E. N., and Spudich, J. L. (2001) Crystal structure of sensory rhodopsin II at 2.4 Å: Insights into color tuning and transducer interaction, *Science 293*, 1499−1503.
57. Royant, A., Nollert, P., Edman, K., Neutze, R., Landau, E. M., Pebay-Peyroulla, E., and Navarro, J. (2001) X-ray structure of sensory rhodopsin II at 2.1-Å resolution, *Proc. Natl. Acad. Sci. U.S.A. 98*, 10131−10136.
58. Kolbe, M., Besir, H., Essen, L. O., and Oesterhelt, D. (2000) Structure of the light-drive chloride pump halorhodopsin at 1.8 Å resolution, *Science 288*, 1390−1396.
59. Mogi, T., Stern, L. J., Marti, T., Chao, B. H., and Khorana, H. G. (1988) Aspartic acid substitutions affect proton translocation by bacteriorhodopsin, *Proc. Natl. Acad. Sci. U.S.A. 85*, 4148−4152.
60. Kandori, H., Kinoshita, N., Yamazaki, Y., Maeda, A., Shichida, Y., Needleman, R., Lanyi, J. K., Bizounok, M., Herzfeld, J., Raap, J., and Lugtenburg, J. (1999) Structural change of threonine 89 upon photoisomerization in bacteriorhodopsin as revealed by polarized FTIR spectroscopy, *Biochemistry 38*, 9676−9683.
61. Kandori, H., Yamazaki, Y., Shichida, Y., Raap, J., Lugtenburg, J., Belenky, M., and Herzfeld, J. (2001) Tight Asp-85-Thr-89 association during the pump switch of bacteriorhodopsin, *Proc. Natl. Acad. Sci. U.S.A. 98*, 1571−1576.
62. Kandori, H., Belenky, M., and Herzfeld, J. (2002) Vibrational frequency and dipolar orientation of the protonated Schiff base in bacteriorhodopsin before and after photoisomerization, *Biochemistry 41*, 6026−6031.
63. Thompson, J. D., Higgins, D. G., and Gibson, T. J. (1994) CLUSTAL W: Improving the sensitivity of progressive multiple sequence alignment through sequence weighting, position-specific gap penalties, and weight matrix choice, *Nucleic Acids Res. 22*, 4673−4680.

BI049158C